Synthesis and Reactivity of the 13-Vertex Metallacarborane Anions [4,4,4-$(CO)_3$-*closo*-4,1,6-$MC_2B_{10}H_{12}]^-$ (M = Re, Mn)

Bruce E. Hodson, Thomas D. McGrath, and F. Gordon A. Stone*

Department of Chemistry and Biochemistry, Baylor University, Waco, Texas 76798-7348

Received March 23, 2005

Reaction of Na_2[*nido*-7,9-$C_2B_{10}H_{12}$] with either [$ReBr(CO)_3(THF)_2$] or [$Mn(NCMe)_3(CO)_3$][PF_6] in THF (THF = tetrahydrofuran), followed by introduction of [$N(PPh_3)_2$]Cl, affords the 13-vertex monoanionic metallacarboranes [$N(PPh_3)_2$][4,4,4-$(CO)_3$-*closo*-4,1,6-$MC_2B_{10}H_{12}$] (M = Re (**2a**), Mn (**2b**), respectively). Treatment of **2a** with I_2 results in iodide substitution at a cage {BH} vertex to form [$N(PPh_3)_2$][4,4,4-$(CO)_3$-7-I-*closo*-4,1,6-$ReC_2B_{10}H_{11}$] (**3**), which, upon reaction with MeMgBr, gives the methylated derivative [$N(PPh_3)_2$][4,4,4-$(CO)_3$-7-Me-*closo*-4,1,6-$ReC_2B_{10}H_{11}$] (**4**). Treatment of **2a** with [NO][BF_4] in CH_2Cl_2 forms two species, [4,4-$(CO)_2$-4-NO-7-X-*closo*-4,1,6-$ReC_2B_{10}H_{11}$] (X = H (**5**), Cl (**6**)). Bimetallic compounds are formed upon treatment of **2a** with 1 molar equiv of the cations $\{M'(PPh_3)\}^+$, namely, the zwitterionic species [4,4,4-$(CO)_3$-4,7-{M′(PPh_3)}-7-(μ-H)-*closo*-4,1,6-$ReC_2B_{10}H_{11}$] (M′ = Cu (**7**), Au (**8**)). A novel, dicopper species, [4-PPh_3-4,7,10-{$Cu(PPh_3)$}-7,10-(μ-$H)_2$-*closo*-4,1,6-$CuC_2B_{10}H_{10}$] (**9**), has been isolated during the synthesis of **7**.

Introduction

We have recently reported the synthesis of the 13-vertex metallacarboranes [NEt_4][4-(η^3-C_3H_5)-*closo*-4,1,6-$NiC_2B_{10}H_{12}$] and [$N(PPh_3)_2$][4-(1,2:5,6-η-C_8H_{12})-*closo*-4,1,6-$RhC_2B_{10}H_{12}$] (vertexes are numbered as in Chart 1), which were shown to react with monocationic metal ligand fragments to form bimetallic species in which the exo-polyhedral metal center M generally is bound to the cluster solely by B−H→M agostic-type interactions.[1] In the nickel system, unfortunately, ligand substitution at the nickel vertex via protonation of the allyl group in the presence of a suitable donor led only to decomposition.[1a] This sensitivity to protonation also precluded many of the cage substitution reactions common in related 12-vertex {*closo*-3,1,2-MC_2B_9} systems.[2] In parallel with this, protonation of the rhodacarborane anion also took place at the metal-bound organic ligand but gave a stable {η^3-C_8H_{13}} moiety that enjoyed additional agostic C−H···Rh bonding.[1b] Contrarily, the same parent anion with other hydride-abstracting agents in the presence of a donor L was shown to undergo {B−H}$^-$ → {B−L} substitution as seen in 12-vertex systems.[2]

The 12-vertex rhenacarborane anion [3,3,3-$(CO)_3$-*closo*-3,1,2-$ReC_2B_9H_{11}]^-$ (**1a**) (Chart 2) was first synthesized by Hawthorne and co-workers several decades ago[3] via reaction of Na_2[*nido*-7,8-$C_2B_9H_{11}$] and [$ReBr(CO)_5$] in THF. More recently, this rhenacarborane has been the subject of renewed study,[4−6] and a variety of bimetallic species have been prepared by reaction with monocationic metal ligand fragments. Among the products are examples of zwitterionic compounds in which an exo-polyhedral metal fragment M′ is attached by a

Chart 1

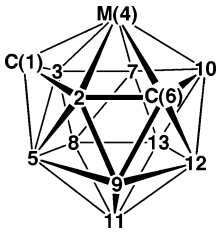

Chart 2

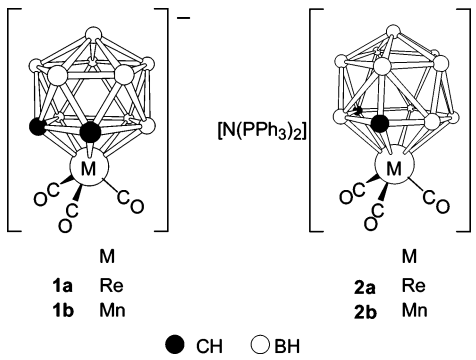

* To whom correspondence should be addressed. E-mail: gordon_stone@baylor.edu.

(1) (a) Hodson, B. E.; McGrath, T. D.; Stone, F. G. A. *Dalton Trans.* **2004**, 2570. (b) Hodson, B. E.; McGrath, T. D.; Stone, F. G. A. *Organometallics* **2005**, *24*, 1638.

(2) Examples include: (a) Brew, S. A.; Stone, F. G. A. *Adv. Organomet. Chem.* **1993**, *35*, 135. (b) Jelliss, P. A.; Stone, F. G. A. *J. Organomet. Chem.* **1995**, *500*, 307. (c) Hata, M.; Kautz, J. A.; Lu, X. L.; McGrath, T. D.; Stone, F. G. A. *Organometallics* **2004**, *23*, 3590. (d) McGrath, T. D.; Stone, F. G. A. *Adv. Organomet. Chem.* **2005**, *53*, in press.

(3) (a) Hawthorne, M. F.; Andrews, T. D. *J. Am. Chem. Soc.* **1965**, *87*, 2496. (b) Andrews, T. D.; Hawthorne, M. F.; Howe, D. V.; Pilling, R. L.; Pitts, D.; Reintjes, M.; Warren, L. F.; Wegner, P. A.; Young, D. C. *J. Am. Chem. Soc.* **1968**, *90*, 879.

(4) Ellis, D. D.; Jelliss, P. A.; Stone, F. G. A. *Organometallics* **1999**, *18*, 4982.

(5) (a) Ellis, D. D.; Jelliss, P. A.; Stone, F. G. A. *J. Chem. Soc., Dalton Trans.* **2000**, 2113. (b) Ellis, D. D.; Jeffery, J. C.; Jelliss, P. A.; Kautz, J. A.; Stone, F. G. A. *Inorg. Chem.* **2001**, *40*, 2041.

10.1021/om050226g CCC: $30.25
Publication on Web 05/27/2005

Table 1. Analytical and Physical Data[a]

cmpd	yield (%)	ν_{max}(CO)[b]/cm^{-1}	anal.[c] (%) C	H	N
$[N(PPh_3)_2][4,4,4\text{-}(CO)_3\text{-}closo\text{-}4,1,6\text{-}ReC_2B_{10}H_{12}]$ (**2a**)	60	2019 s, 1931 s br	51.9 (51.7)	4.5 (4.4)	1.2 (1.5)
$[N(PPh_3)_2][4,4,4\text{-}(CO)_3\text{-}closo\text{-}4,1,6\text{-}MnC_2B_{10}H_{12}]$ (**2b**)	25	2011 s, 1932 s br	55.9 (55.6)[d]	5.0 (4.9)	1.8 (1.5)
$[N(PPh_3)_2][4,4,4\text{-}(CO)_3\text{-}7\text{-}I\text{-}closo\text{-}4,1,6\text{-}ReC_2B_{10}H_{11}]$ (**3**)	35	2027 s, 1939 s br	45.5 (45.6)	3.8 (3.8)	1.4 (1.3)
$[N(PPh_3)_2][4,4,4\text{-}(CO)_3\text{-}7\text{-}Me\text{-}closo\text{-}4,1,6\text{-}ReC_2B_{10}H_{11}]$ (**4**)	10	2017 s, 1932 s br	52.2 (52.2)	4.5 (4.6)	1.5 (1.5)
$[4,4\text{-}(CO)_2\text{-}4\text{-}NO\text{-}closo\text{-}4,1,6\text{-}ReC_2B_{10}H_{12}]$ (**5**)	22	2108 s, 2065 s	11.8 (11.5)	2.9 (2.9)	3.4 (3.4)
$[4,4\text{-}(CO)_2\text{-}4\text{-}NO\text{-}7\text{-}Cl\text{-}closo\text{-}4,1,6\text{-}ReC_2B_{10}H_{11}]$ (**6**)	21	2109 s, 2067 s	11.0 (10.7)	2.5 (2.5)	3.2 (3.1)
$[4,4,4\text{-}(CO)_3\text{-}4,7\text{-}\{Cu(PPh_3)\}\text{-}7\text{-}(\mu\text{-}H)\text{-}closo\text{-}4,1,6\text{-}ReC_2B_{10}H_{11}]$ (**7**)	60	2039 s, 1945 s br	37.6 (37.3)	3.8 (3.7)	
$[4,4,4\text{-}(CO)_3\text{-}4,7\text{-}\{Au(PPh_3)\}\text{-}7\text{-}(\mu\text{-}H)\text{-}closo\text{-}4,1,6\text{-}ReC_2B_{10}H_{11}]$ (**8**)	47	2020 s, 1932 s br	31.2 (31.6)	3.4 (3.1)	

[a] All compounds are yellow, except **4**, which is yellow-brown, and **9**, which is almost colorless (very pale yellow). [b] Measured in CH_2Cl_2; all spectra show a broad, medium-intensity band at ca. 2550 cm^{-1} due to B−H absorptions. In addition, ν_{max}(NO)/cm^{-1}: for **5**, 1812 br s; for **6**,1814 br s. [c] Calculated values are given in parentheses. [d] Crystallizes with 1.0 molar equiv of CH_2Cl_2.

combination of a direct Re−M′ bond and supporting B−H→M′ agostic interaction(s)[5] or by multiple agostic interactions alone.[4] In addition, the cluster of **1a** has been shown to be susceptible to substitution at both the rhenium and boron vertexes under suitable conditions.[6] Treatment with [NO][BF_4] results in loss of one CO ligand and formation of the neutral species $[3,3\text{-}(CO)_2\text{-}3\text{-}NO\text{-}closo\text{-}3,1,2\text{-}ReC_2B_9H_{11}]$.[6a] Halogen substitution is also possible,[6c,d] and several of these substituted species show interesting optical and electronic properties.[6b−d] The anion **1b**, a manganese analogue of **1a**, has similarly long been known.[3] Only very recently, however, has the chemistry of this manganacarborane been explored in any depth,[2c] when it was shown also to enjoy a rich reactivity.

The versatility of compounds **1** suggested that 13-vertex analogues would possess a similar wealth of chemistry. Although a "full-sandwich" 13-vertex manganacarborane $[Mn(C_2B_{10}H_{12})_2]^{2-}$ has been described,[7] it was reported that an attempted synthesis of the "half-sandwich" direct analogue of **1b** using $Na_2[nido\text{-}7,9\text{-}C_2B_{10}H_{12}]$ and [$MnBr(CO)_5$] was unsuccessful.[8] However, use of the complex [$ReBr(CO)_3(THF)_2$] has been shown to improve yields of **1a** by over 30% in comparison to use of [$ReBr(CO)_5$];[4] the former reagent has also been effectively applied in the synthesis of $\{ReCB_{10}\}$[9,10] and $\{ReCB_9\}$[11] cage systems. Likewise, we have successfully used a related manganese compound, $[Mn(NCMe)_3(CO)_3][PF_6]$, to improve yields of **1b**[2c] and in the preparation of $\{MnCB_9\}$ species.[12] By reaction of these alternate metal synthons with $Na_2[nido\text{-}7,9\text{-}C_2B_{10}H_{12}]$ we have been able to prepare the 13-vertex rhena- and mangana-carborane anions $[4,4,4\text{-}(CO)_3\text{-}closo\text{-}4,1,6\text{-}MC_2B_{10}H_{12}]^-$ (M = Re or Mn), upon which we now report.

Results and Discussion

Addition of $Na_2[nido\text{-}7,9\text{-}C_2B_{10}H_{12}]$[13] to a hot THF solution of [$ReBr(CO)_3(THF)_2$], with subsequent addition of $[N(PPh_3)_2]Cl$, results in formation of the 13-vertex rhenacarborane $[N(PPh_3)_2][4,4,4\text{-}(CO)_3\text{-}closo\text{-}4,1,6\text{-}ReC_2B_{10}H_{12}]$ (**2a**). The analogous manganacarborane $[N(PPh_3)_2][4,4,4\text{-}(CO)_3\text{-}closo\text{-}4,1,6\text{-}MnC_2B_{10}H_{12}]$ (**2b**) was obtained similarly, using $[Mn(NCMe)_3(CO)_3][PF_6]$ as the transition metal reagent. Data characterizing compounds **2** are presented in Tables 1 and 2. Their carbonyl groups showed strong absorbances in IR spectra at 2019 and 1931 cm^{-1} (**2a**) and at 2011 and 1932 cm^{-1} (**2b**). These may be compared with the corresponding data for the $[N(PPh_3)_2]^+$ salts of their 12-vertex analogues, which show similar IR absorbances at 2008 and 1910 cm^{-1} (**1a**) and at 2002 and 1916 cm^{-1} (**1b**). This provides a preliminary comparison of the differing donor characteristics of $\{C_2B_{10}\}$ versus $\{C_2B_9\}$ ligands, although other details of the metals' and the ligands' frontier electronic properties will also be involved.

The metal-bound carbonyl ligands resonate at δ 192.8 (**2a**) and 220.2 (**2b**) in the $^{13}C\{^1H\}$ NMR spectra, with the carborane CH units appearing as broad signals at δ 3.11 (**2a**) and 2.87 (**2b**) in their ^1H NMR spectra and at δ 46.1 (**2a**) and 39.5 (**2b**) in their $^{13}C\{^1H\}$ NMR spectra. The appearance of only a single resonance in each spectrum for the cage CH group is indicative of the anion possessing pseudo-C_s symmetry in solution.[8] This is also supported by the compounds' $^{11}B\{^1H\}$ NMR spectra, which show a 1:3(2+1 coincidence):2:1:2:1 intensity ratio in the spectrum of **2a** and a similar pattern in that of **2b**.

Single-crystal X-ray diffraction studies of compounds **2** revealed molecular structures as shown in Figure 1 for **2b**. As is to be expected, the two compounds afforded isomorphous crystals and their anions have very similar structures with the obvious exception of the two metals' differing radii. Thus, in both anions the metal atom caps the six-atom CBCBBB open face of the *nido* carborane unit, while the three carbonyl ligands complete a "piano stool" arrangement. The cage carbon atoms C(1) and C(6) are, respectively, 4- and 5-connected in the solid state, a situation typical in 13-vertex $\{closo\text{-}4,1,6\text{-}MC_2B_{10}\}$ clusters. Both structures suffer from some disorder associated with B(5), and we note that similar

(6) (a) Ellis, D. D.; Jelliss, P. A.; Stone, F. G. A. *Chem. Commun.* **1999**, 2385. (b) Bitterwolf, T. E.; Scallorn, W. B.; Weiss, C. A.; Jelliss, P. A. *Organometallics* **2002**, *21*, 1856. (c) Fischer, M. J.; Jelliss, P. A.; Phifer, L. M.; Rath, N. P. *Inorg. Chim. Acta* **2005**, *358*, 1531. (d) Fischer, M. J.; Jelliss, P. A.; Orlando, J. H.; Phifer, L. M.; Rath, N. P. *J. Lumin.* **2005**, in press.
(7) Salentine, C. G.; Hawthorne, M. F. *Inorg. Chem.* **1976**, *15*, 2872.
(8) Dustin, D. F.; Dunks, G. B.; Hawthorne, M. F. *J. Am. Chem. Soc.* **1973**, *95*, 1109.
(9) Blandford, I.; Jeffery, J. C.; Jelliss, P. A.; Stone, F. G. A. *Organometallics* **1998**, *17*, 1402.
(10) Du, S.; Kautz, J. A.; McGrath, T. D.; Stone, F. G. A. *Chem. Commun.* **2002**, 1004.
(11) Du, S.; Kautz, J. A.; McGrath, T. D.; Stone, F. G. A. *Organometallics* **2003**, *22*, 2842.
(12) Du, S.; Farley, R. B.; Harvey, J. N.; Jeffery, J. C.; Kautz, J. A.; Maher, J. P.; McGrath, T. D.; Murphy, D. M.; Riis-Johannessen, T.; Stone, F. G. A. *Chem. Commun.* **2003**, 1846.
(13) Callahan, K. P.; Hawthorne, M. F. *Adv. Organomet. Chem.* **1976**, *14*, 145.

Table 2. ^{1}H, ^{13}C, ^{11}B, and ^{31}P NMR Data[a]

cmpd	$^{1}H/\delta$[b]	$^{13}C/\delta$[c]	$^{11}B/\delta$[d]
2a	7.88−7.43 (m, 30H, Ph), 3.11 (br s, 2H, cage CH)	192.8 (CO), 134.1−125.8 (Ph), 46.1 (br, cage CH)	0.8, −0.6 (3B), −7.5 (2B), −8.6, −14.5 (2B), −21.2
2b	7.78−7.42 (m, 30H, Ph), 2.87 (br s, 2H, cage CH)	220.2 (CO), 133.9−124.8 (Ph), 39.5 (br, cage CH)	5.5, 1.8 (2B), 0.1, −6.0 (3B), −13.1 (2B), −19.1
3	7.85−7.51 (m, 30H, Ph), 3.23 (br s, 2H, cage CH)	191.8 (CO), 133.8−125.3 (Ph), 45.1 (br, cage CH)	−0.2 (4B), −5.3 (2B), −13.6 (B(7)), −14.3 (2B), −21.8
4	7.73−7.42 (m, 30H, Ph), 2.98 (br s, 2H, cage CH), 0.74 (br s, 3H, Me)	193.4 (CO), 133.8−126.4 (Ph), 44.5 (br, cage CH), 27.4 (Me)	10.8 (B(7)), 1.2 (2B), −0.6, −5.1 (2B), −9.2, −14.1 (2B), −24.6
5	4.26 (br s, 2H, cage CH)	180.0 (CO), 59.1 (br, cage CH)	7.6, 4.7 (2B), 3.4, 0.0 (2B), −4.1, −10.6 (3B)
6	4.16 (br s, 2H, cage CH)	179.3 (CO), 58.8 (br, cage CH)	14.6 (B(7)), 3.5 (2B), 1.6 (3B), −1.1, −11.6 (2B), −14.8
7[e]	7.62−7.24 (m, 15H, Ph), 3.50 (br s, 2H, cage CH)	188.2 (CO), 134.0−129.6 (Ph), 49.2 (br, cage CH)	3.8, −4.7, −6.4, −9.3 (2B), −10.2 (2B), −13.5 (2B), −16.9
8[e]	7.66−7.25 (m, 15H, Ph), 3.10 (br s, 2H, cage CH)	192.5 (CO), 134.5−126.2 (Ph), 46.8 (br, cage CH)	1.3, −1.1 (3B), −7.5 (3B), −14.6 (2B), −20.4
9[e]	7.47−7.22 (m, 30H, Ph), 4.39 (br s, 2H, cage CH)	134.1−129.1 (Ph), 78.2 (br, cage CH)	1.4 (vbr), −5.6, −7.0, −9.3 (2B), −11.5, −16.9 (2B), −19.1 (2B)

[a] Chemical shifts (δ) in ppm; measurements at ambient temperatures in CD_2Cl_2. [b] Resonances for terminal BH protons occur as broad unresolved signals in the range δ ca. −1 to +3. [c] ^{1}H-decoupled chemical shifts are positive to high frequency of $SiMe_4$. [d] ^{1}H-decoupled chemical shifts are positive to high frequency of $BF_3{\cdot}OEt_2$ (external); resonances are of unit integral except where indicated. [e] $^{31}P\{^{1}H\}$ NMR (positive to high frequency of 85% H_3PO_4 (external)): for **7**, δ 10.4 (br); for **8**, δ 34.6 (br); for **9**, δ 8.3 (br), 7.2 (br).

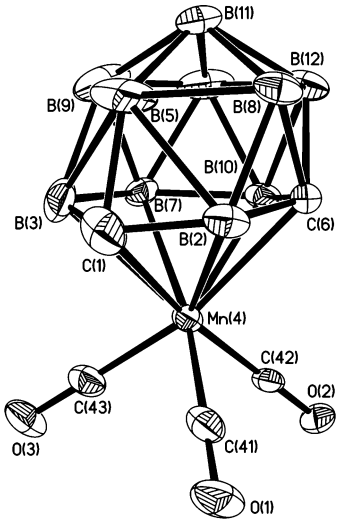

Figure 1. Structure of the anion of **2b** showing the crystallographic labeling scheme; the geometry of the anion of **2a** is very similar. In this and subsequent figures, thermal ellipsoids are drawn at the 40% probability level, and for clarity only the *ipso* carbons of phenyl rings and only chemically significant hydrogen atoms are shown. Selected bond lengths (Å) and angles (deg) for **2a**: C(1)−Re(4) 2.293(3), B(2)−Re(4) 2.391(4), B(3)−Re(4) 2.416(4), C(6)−Re(4) 2.387(3), B(7)−Re(4) 2.361(3), B(10)−Re(4) 2.341(3), Re(4)−C(41) 1.928(3), Re(4)−C(42) 1.941(3), Re(4)−C(43) 1.922(3); C(41)−Re(4)−C(42) 89.25(12), C(43)−Re(4)−C(41) 90.19(13), C(43)−Re(4)−C(42) 91.06(12). For **2b**: C(1)−Mn(4) 2.153(3), B(2)−Mn(4) 2.270(3), B(3)−Mn(4) 2.316(3), C(6)−Mn(4) 2.279(2), B(7)−Mn(4) 2.259(3), B(10)−Mn(4) 2.228(3), Mn(4)−C(41) 1.815(3), Mn(4)−C(42) 1.802(2), Mn(4)−C(43) 1.794(3); C(42)−Mn(4)−C(41) 88.56(11), C(43)−Mn(4)−C(41) 91.20(11), C(43)−Mn(4)−C(42) 89.86(11).

(albeit more severe) problems have been reported in the structural determinations of related 13-vertex metallacarborane species.[14] This disorder notwithstanding, the two determinations are otherwise unremarkable but do serve to confirm the identities of compounds **2** and in particular that they are the expected 4,1,6-MC_2B_{10} isomers.[14] As compound **2a** was obtained in superior yields and **2b**, moreover, was somewhat less stable, the former was chosen for the further reactivity studies described below. Nevertheless, it should be noted that preliminary experiments upon compound **2b** show very similar reactivity to **2a**, as is to be expected, especially given the rich variety of products reported earlier for the analogous 12-vertex species **1b**.[2c]

Chart 3

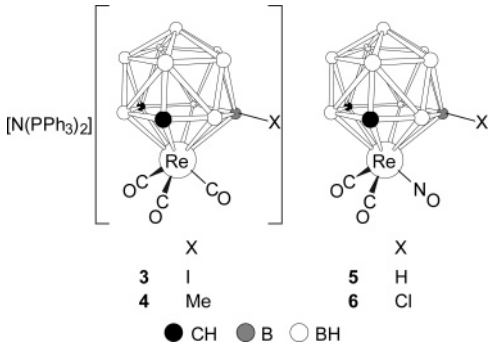

Treatment of compound **2a** with I_2 in CH_2Cl_2 results in the substitution of a cage hydride by iodide to form $[N(PPh_3)_2][4,4,4\text{-}(CO)_3\text{-}7\text{-}I\text{-}closo\text{-}4,1,6\text{-}ReC_2B_{10}H_{11}]$ (**3**) (Chart 3), analogous to the products obtained from reaction of compounds **1** with I_2.[2c,6d] An $^{11}B\{^{1}H\}$ NMR spectroscopic study of **3** revealed five resonances in intensity ratio 4:2:1:2:1, with one peak of unit integral, at δ −13.6, remaining a singlet in the corresponding proton-coupled spectrum, indicating substitution to have occurred at this boron vertex. The ^{1}H and $^{13}C\{^{1}H\}$ NMR spectra each showed one broad peak due to the cage CH groups at δ 3.23 (^{1}H) and 45.1 (^{13}C), respectively. The former was of relative integral 2, indicating that the cluster retained mirror symmetry (at least on the NMR time scale) upon substitution. A singlet peak at δ 191.8 due to the carbonyl groups is also seen in the latter spectrum. Unfortunately, diffraction quality crystals of **3** were not obtained, and hence the site of the substituted boron vertex could not be established with certainty.

(14) Burke, A.; McIntosh, R.; Ellis, D.; Rosair, G. M.; Welch, A. J. *Collect. Czech. Chem. Commun.* **2002**, *67*, 991.

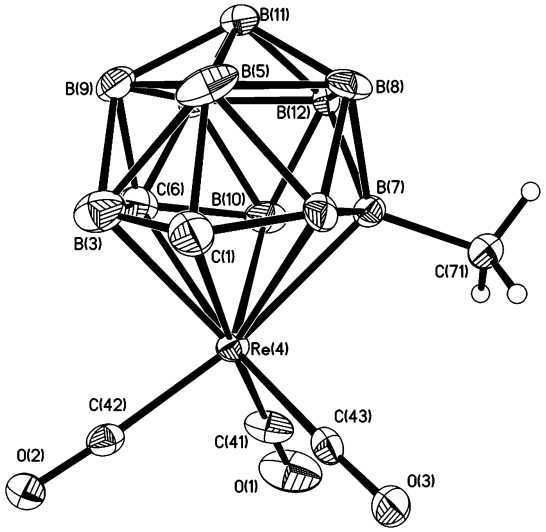

Figure 2. Structure of the anion of **4** showing the crystallographic labeling scheme. Selected bond lengths (Å) and angles (deg): C(1)−Re(4) 2.262(3), B(2)−Re(4) 2.398(3), B(3)−Re(4) 2.429(4), C(6)−Re(4) 2.362(3), B(7)−Re(4) 2.442(3), B(10)−Re(4) 2.327(3), Re(4)−C(41) 1.924(3), Re(4)−C(42) 1.947(3), Re(4)−C(43) 1.921(3), B(7)−C(71) 1.605(4); C(41)−Re(4)−C(42) 88.11(13), C(43)−Re(4)−C(42) 92.81(11), C(43)−Re(4)−C(41) 86.35(14), C(71)−B(7)−Re(4) 117.26 (18).

Introduction of a 15-fold excess of MeMgBr to a THF solution of freshly prepared **3** resulted in substitution of the iodide by a methyl group to form $[N(PPh_3)_2][4,4,4\text{-}(CO)_3\text{-}7\text{-}Me\text{-}closo\text{-}4,1,6\text{-}ReC_2B_{10}H_{11}]$ (**4**). The ^{11}B NMR spectrum of **4** (Table 2) revealed a nonproton-coupled peak at δ 10.8, a significant downfield shift compared with the corresponding peak in **3** (observed at δ −13.6). This peak is assigned as the methyl-substituted boron vertex, and it is noted that similar shifts have been observed in B−Me versus B−I derivatives of **1b** (δ 5.3 versus −14.8).[2c] The methyl group in **4** is evident in the ^1H NMR spectrum as a broad singlet peak at δ 0.74 and in the $^{13}C\{^1H\}$ NMR spectrum as a broad resonance at δ 27.4.

An X-ray crystallographic study of **4** (Figure 2) showed that the rhenium atom is coordinated by the carborane cage in a manner very similar to that observed in **2a**, with the carbonyl groups analogously distributed. A methyl group in **4** is attached to B(7) (B(7)−C(71) is 1.605(4) Å), implying that the initial site of iodide substitution in **3** was also B(7), reasonably assuming that no iodide migration about the metallacarborane surface had occurred. The B(7) position is in a site that is β with respect to the carbon atoms in the ligating $\overline{CBCB}B\overline{B}$ face. This vertex is intuitively favored for substitution due to its proximity to the metal atom and distance from the relatively electronegative carbon atoms in the carborane face. Although the anion of **4** (and, by implication, **3**) is asymmetric in the solid state, fluxional processes render the two cage-carbon atoms equivalent, and hence the cluster has time-averaged C_s symmetry in solution.[8] The formation of **4** suggests that a large number of derivative compounds may be similarly synthesized from **3** through use of appropriate Grignard reagents.[2c]

Treatment of **2a** with $[NO][BF_4]$ in CH_2Cl_2 results in loss of a carbonyl ligand and formation of an approximately 1:1 mixture of the substituted products $[4,4\text{-}(CO)_2\text{-}4\text{-}NO\text{-}7\text{-}X\text{-}closo\text{-}4,1,6\text{-}ReC_2B_{10}H_{11}]$ (X = H (**5**), Cl (**6**)), which were conveniently separated by preparative thin-layer chromatography. The reagent $[NO][BF_4]$ has previously been reported to act as a hydride-abstracting agent in metallacarborane systems,[2c,15] and so the simultaneous formation of the two products, compounds **5** and **6**, was not altogether surprising. Removal of H^- from a boron vertex in the anion of **2a**, followed by scavenging of Cl^- from the CH_2Cl_2 solvent, would give the 7-Cl analogue of compound **3**. Evidently the rhenium and BH(7) sites successfully compete for reaction with the nitrosonium cation. This intermediate chlorinated anion presumably is more resistant to further hydride abstraction, but it can react with further $[NO]^+$, undergoing substitution at rhenium—and the anion of **2a** does likewise—to give the observed products.

Data characterizing the two species are collected in Tables 1 and 2. Both compounds showed two strong CO bands in their IR spectra (ν_{max} 2108, 2065 (**5**) and 2109, 2067 (**6**) cm^{-1}), along with a band assigned as an NO stretch at ν_{max} 1812 (**5**) and 1814 (**6**) cm^{-1}. These may be compared with the same bands in an analogous derivative of **1a** (ν_{max} 2093, 2034, and 1776 cm^{-1}, respectively).[6a] The $^{11}B\{^1H\}$ NMR spectrum of **5** displayed six peaks in intensity ratio 1:2:1:2:1:3(2+1 coincidence), again indicating that C_s symmetry is retained in solution. The same spectrum for **6** showed a similar intensity pattern, but the highest frequency resonance (at δ 14.6) remains a singlet upon retention of ^1H coupling and is therefore assigned as the B−Cl-substituted vertex. In the ^1H NMR spectra of **5** and **6** only one broad singlet peak, at δ 4.26 (**5**) and 4.16 (**6**), respectively, is seen for the protons of the carborane cage CH groups. The same units were observed in the corresponding $^{13}C\{^1H\}$ NMR spectra as a broad peak at δ 59.1 (**5**) and 58.8 (**6**), in addition to a sharp peak at δ 180.0 (**5**) and 179.3 (**6**) due to the rhenium-bound carbonyl ligands.

Single crystals of **6** were analyzed by X-ray diffraction, revealing the molecular structure shown in Figure 3. As can be seen, B(7) is confirmed to carry a chloride substituent derived from the CH_2Cl_2 solvent, with the B(7)−Cl(7) separation being 1.829(5) Å; the corresponding distance in the second, crystallographically independent, molecule is essentially identical at 1.836(5) Å. The $\{Re(CO)_2(NO)\}$ unit is orientated such that the nitrosyl ligand is approximately transoid to C(1): N(4)−Re(4)−C(1) is 174.42(12)° and 175.62(12)° in the two crystallographically independent molecules of **6**. Overall the metallacarborane core shows only slight geometric differences compared with that in **2a**.

However, the most notable feature of the solid-state structure of compound **6** is illustrated in Figure 4. Within each of the sets of crystallographically independent molecules of **6** (designated molecules **A** and **B**) there are weak hydrogen-bonding interactions between adjacent molecules in the same set, resulting in alternating one-dimensional "chains" (**A**) and two-dimensional "sheets" (**B**) that lie parallel to the crystallographic *a* axis and *ab* plane, respectively. Thus, in each of the molecules **A** the protonic hydrogen atom bound

(15) Ellis, D. D.; Franken, A.; Jelliss, P. A.; Stone, F. G. A.; Yu, P.-Y. *Organometallics* **2000**, *19*, 1993.

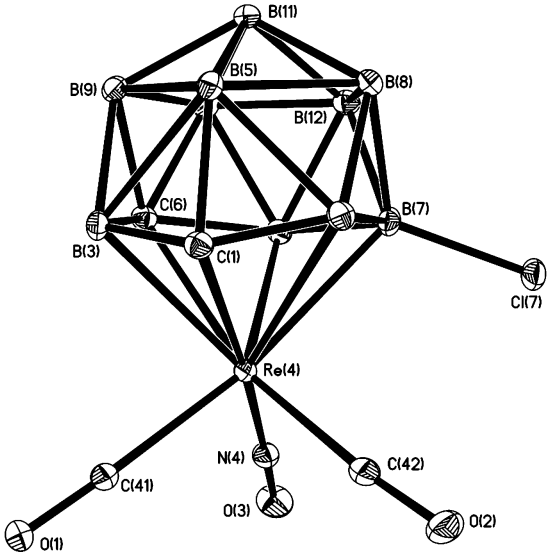

Figure 3. Structure of one of the crystallographically independent molecules of compound **6** showing the crystallographic labeling scheme; the other molecule is very similar (see text). Selected bond lengths (Å) and angles (deg): C(1)−Re(4) 2.226(3), B(2)−Re(4) 2.472(3), B(3)−Re(4) 2.400(3), C(6)−Re(4) 2.383(3), B(7)−Re(4) 2.405(5), B(10)−Re(4) 2.319(3), Re(4)−C(41) 2.024(3), Re(4)−C(42) 1.984(3), Re(4)−N(4) 1.822(3), B(7)−Cl(7) 1.829(5); N(4)−Re(4)−C(1) 174.42(12), N(4)−Re(4)−C(41) 90.31(12), N(4)−Re(4)−C(42) 91.64(13), C(41)−Re(4)−C(42) 92.21(13), Cl(7)−B(7)−Re(4) 115.1(2).

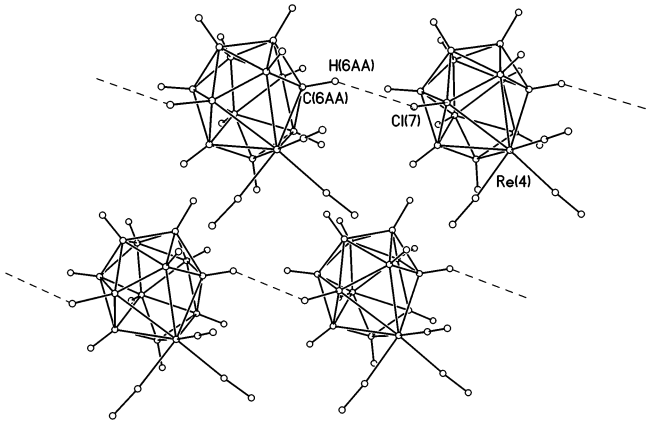

Figure 4. Packing of one of the crystallographically independent molecules (**A**) of compound **6** along the crystallographic *a* direction, illustrating some of the B−Cl···H−C interactions in the solid state. The distance Cl(7)···H(6AA) is 2.80(5) Å and Cl(7)···C(6AA) is 3.699(4) Å; the Cl(7)···H(6AA)−C(6AA) angle is 145(3)°.

to C(6) is close to the chloride of an adjacent molecule (crystallographic *a* direction), so that the H···Cl distance is 2.80(5) Å, with the corresponding C···Cl separation being 3.699(4) Å and C−H−Cl being 145(3)°. In the molecules **B**, the comparable CH(6)···Cl distance is somewhat longer, at 3.00(5) Å, but there is an additional similar contact (2.95(5) Å) to CH(1) in another, diagonally adjacent molecule (crystallographic *ab* direction). The H···Cl distances in the present system are essentially identical within experimental error and compare well with other CH···Cl separations in the Cambridge Structural Database.[16] Although carborane C−H···(halogen) interactions are well known,[17] we are only aware of one other example of similar intermolecular C−H···Cl−B contacts in a metallacarborane, where the H···Cl distance is 2.99 Å, with the C−H−Cl angle being 149°.[18]

Chart 4

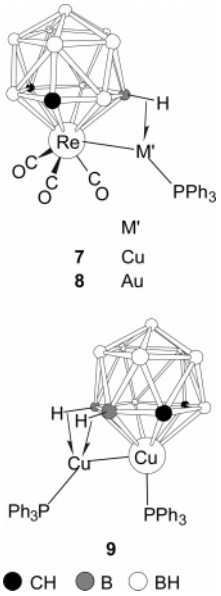

Previous studies upon 13-vertex {*closo*-4,1,6-MC_2B_{10}} systems have shown that an exo-polyhedral metal fragment (M′) can be attached to the cluster via direct M−M′ bonds, B−M′ bonds, and/or one or more B−H→M′ agostic interactions. However, only a somewhat limited range of such species exists.[1,19−21] Given the many examples of bimetallic species derived from the anion **1a**,[4,5] and the few recently also reported from **1b**,[2c] it was clearly of interest to search for similar derivatives of **2a**. Reactions of compounds **2** with a number of transition metal cations resulted only in decomposition, typically via redox reactions that eliminated the *nido* carborane ligand as its neutral *closo* parent. However, with sources of the cations $\{M'(PPh_3)\}^+$ (M′ = Cu, Au), bimetallic species were successfully obtained. Thus, dissolution of **2a** in THF, followed by addition of either $[CuCl(PPh_3)]_4$ or $[AuCl(PPh_3)]$ and $Tl[PF_6]$, yielded the neutral bimetallic species [4,4,4-$(CO)_3$-4,7-{M′(PPh_3)}-7-(μ-H)-*closo*-4,1,6-$ReC_2B_{10}H_{11}$] (M′ = Cu (**7**), Au (**8**)) (Chart 4). The formation of compound **8** may be somewhat anomalous in that whereas the 12-vertex analogue of compound **7**, namely, [3,3,3-$(CO)_3$-3,8-{$Cu(PPh_3)$}-8-(μ-H)-*closo*-3,1,2-$ReC_2B_9H_{10}$], is readily obtained from **1a**, the corresponding {Au-ReC_2B_9} species purportedly does not form.[4] However, both the Cu−Mn and Au−Mn derivatives of **1b** are known.[2c]

Characterizing data for compounds **7** and **8** are contained in Tables 1 and 2. Compound **7** displays two absorptions in its IR spectrum due to the CO ligands,

(16) Allen, F. H. *Acta Crystallogr.* **2002**, *B58*, 388. Bruno, I.; Cole, J. C.; Edgington, P. R.; Kessler, M.; Macrae, C. F.; McCabe, P.; Pearson, J.; Taylor, R. *Acta Crystallogr.* **2002**, *B58*, 389.
(17) Fox, M. A.; Hughes, A. K. *Coord. Chem. Rev.* **2004**, *248*, 457.
(18) Konoplev, V. E.; Pisareva, I. V.; Lemenovskii, D. I.; Petrovskii, P. V.; Tok, O. L.; Dolgushin, F. M.; Chizhevsky, I. T. *Collect. Czech. Chem. Commun.* **2002**, *67*, 936.
(19) Barker, G. K.; Garcia, M. P.; Green, M.; Stone, F. G. A.; Welch, A. J. *J. Chem. Soc., Chem. Commun.* **1983**, 137.
(20) Dossett, S. J.; Mullica, D. F.; Sappenfield, E. L.; Stone, F. G. A.; Went, M. J. *J. Chem. Soc., Dalton Trans.* **1993**, 281.
(21) Carr, N.; Mullica, D. F.; Sappenfield, E. L.; Stone, F. G. A.; Went, M. J. *Organometallics* **1993**, *12*, 4350.

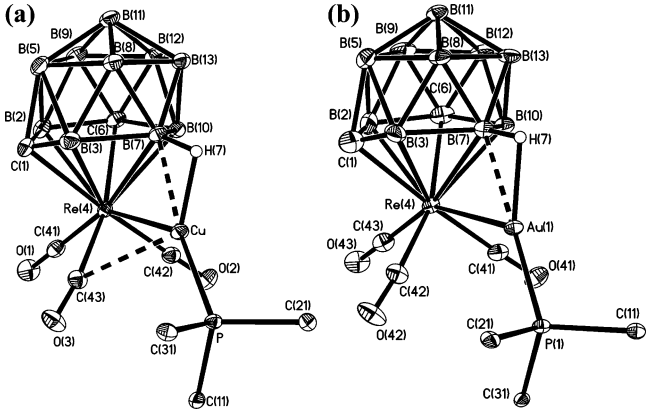

Figure 5. Structures of (a) compound **7** and (b) compound **8** showing the crystallographic labeling schemes. Selected bond lengths (Å) and angles (deg) for **7**: Re(4)−Cu 2.6826(2), C(1)−Re(4) 2.2480(19), B(2)−Re(4) 2.392(2), B(3)−Re(4) 2.463(2), C(6)−Re(4) 2.3820(18), B(7)−Re(4) 2.4434(19), B(10)−Re(4) 2.3643(19), C(43)···Cu 2.5207(17), B(7)−H(7) 1.18(2), B(7)···Cu 2.1399(19), Cu−H(7) 1.66(2), Cu−P 2.2099(5); P−Cu−B(7) 161.24(5), P−Cu−Re(4) 137.875(14), B(7)−Cu−Re(4) 59.63(5). For **8**: Re(4)−Au(1) 2.899(3), C(1)−Re(4) 2.259(7), B(2)−Re(4) 2.328(7), B(3)−Re(4) 2.458(6), C(6)−Re(4) 2.341(6), B(7)−Re(4) 2.411(6), B(10)−Re(4) 2.365(6), B(7)−H(7) 1.12(5), B(7)···Au(1) 2.256(6), Au(1)−H(7) 1.81(5), Au(1)−P(1) 2.226(2); P(1)−Au(1)−B(7) 172.30(14), P(1)−Au(1)−Re(4) 130.77(6), B(7)−Au(1)−Re(4) 54.04(16).

at 2039 and 1945 cm^{-1}, while those for **8** appear at 2020 and 1932 cm^{-1}. Both of these are significantly to higher frequency than the CO stretching frequencies in the anionic compounds **2**−**4**, as would be expected. The $^{11}B\{^1H\}$ NMR spectra of **7** and **8** reveal resonances in the intensity ratios 1:1:1:2:2:2:1 and 1:3:3:2:1, respectively, both suggestive of time-averaged molecular symmetry (assuming integral-3 resonances to be 1+2 coincidences). A broad peak at δ 10.4, typical of PPh_3 coordinated to a copper atom, was evident in the $^{31}P\{^1H\}$ NMR spectrum of **7**; the corresponding moiety bound to gold in **8** resonates at δ 34.6 in the same spectrum. The aromatic region of both compounds' ^1H NMR spectra showed complex sets of multiplets due to the phenyl groups of the PPh_3 ligand in the exo-polyhedral fragment. These were in the ratio 15:2 with the broad resonances at δ 3.50 (**7**) and 3.10 (**8**), respectively, for the cage CH units, confirming only a single PPh_3 unit to be bound to the exo-polyhedral M′ centers. The presence of B−H⇀M′ bonds could not be confirmed in the ^1H NMR spectra, probably due to a rapid exchange of B−H binding sites on the NMR time scale rendering any such peak too broad to be observed.[22] Accordingly, single-crystal X-ray diffraction studies were undertaken to check for the presence of any such interactions.

The structures determined for compounds **7** and **8** are shown in Figure 5. In both molecules, the exo-polyhedral {M′(PPh_3)} fragment is bound to the rhenacarbaborane via a direct Re−M′ bond (Re(4)−Cu = 2.6826(2) Å; Re(4)−Au(1) = 2.899(3) Å) and is supported by a single

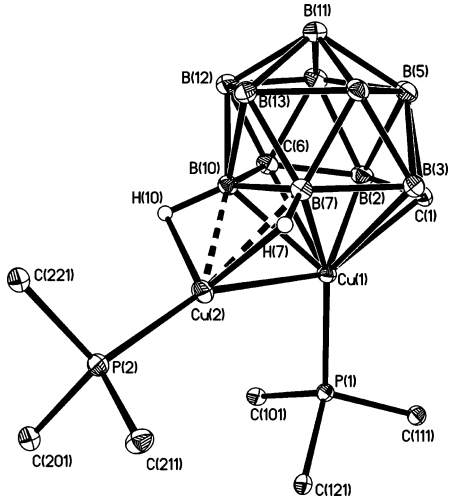

Figure 6. Structure of compound **9** showing the crystallographic labeling scheme. Selected bond lengths (Å) and angles (deg): Cu(1)−Cu(2) 2.6015(3), Cu(1)−C(1) 2.0786(17), Cu(1)−B(2) 2.3017(19), Cu(1)−B(3) 2.2747(19), Cu(1)−C(6) 2.3936(15), Cu(1)−B(7) 2.1992(17), Cu(1)−B(10) 2.1922(16), B(7)···Cu(2) 2.1937(18), Cu(2)−H(7) 1.941(18), B(10)···Cu(2) 2.1807(18), Cu(2)−H(10) 1.928(18); P(1)−Cu(1)−Cu(2) 99.688(15), B(7)−Cu(2)−P(2) 143.99(5), B(10)−Cu(2)−P(2) 145.05(5), P(2)−Cu(2)−Cu(1) 157.067(14).

B−H⇀M′ agostic-type interaction from the β-boron atom in the rhenium-ligating $\overline{\text{CBCBBB}}$ face (Cu···B(7) = 2.1399(19) Å; Au(1)···B(7) = 2.256(6) Å). A very similar geometry was observed in the $\{ReC_2B_9\}$ analogue of **7**, where the corresponding distances are Re−Cu = 2.6583(6) and B···Cu = 2.169(3) Å.[4] In **7**, there is also a close approach between the Cu atom and one carbonyl ligand, though this interaction is sufficiently distant (Cu···C(43) is 2.5207(17) Å) that there is only a slight effect upon the Re(4)−C(43)−O(3) angle (172.74(17)°). The longer Re−Au distance (versus Re−Cu) in **8** places the Au center farther from the Re-bound CO groups, so that the corresponding Au···CO approach is much more distant (over 2.8 Å).

We have observed that on occasion compound **7** as isolated is accompanied by a second metallacarborane product. The two species travel closely together under chromatography and ultimately were only separated by fractional crystallization and manual separation of the two crystal types. This second species is [4-PPh_3-4,7,10-{Cu(PPh_3)}-7,10-(μ-H)$_2$-*closo*-4,1,6-$CuC_2B_{10}H_{10}$] (**9**), whose identity was only established following an X-ray diffraction study. The results are depicted in Figure 6. The molecule is also of the 13-vertex {*closo*-4,1,6-MC_2B_{10}} type and bears an exo-polyhedral {Cu(PPh_3)} unit, but very surprisingly the cluster vertex M is supplied by a second {Cu(PPh_3)} moiety. This endo-polyhedral copper atom (Cu(1)) is bonded essentially symmetrically to the η^6-$\overline{\text{CBCBBB}}$ face of the carborane, some variation in the Cu···C/Cu···B distances being due to puckering of this six-membered face. In addition to this and a PPh_3 ligand Cu(1) is bonded to the exo-polyhedral copper center (Cu(1)−Cu(2) = 2.6015(3) Å). This second copper itself also bears a PPh_3 group and is further supported by two agostic-type B−H⇀Cu interactions (Cu(2)···B(7) = 2.1937(18), Cu(2)···B(10) = 2.1807(18) Å). The two latter features involve one β- and

(22) Cabioch, J.-L.; Dossett, S. J.; Hart, I. J.; Pilotti, M. U.; Stone, F. G. A. *J. Chem. Soc., Dalton Trans.* **1991**, 519. Batten, S. A.; Jeffrey, J. C.; Jones, P. L.; Mullica, D. F.; Rudd, M. D.; Sappenfield, E. L.; Stone, F. G. A.; Wolf, A. *Inorg. Chem.* **1997**, *36*, 2570. Ellis, D. D.; Franken, A.; Jelliss, P. A.; Kautz, J. A.; Stone, F. G. A.; Yu, P.-Y. *J. Chem. Soc., Dalton Trans.* **2000**, 2509.

one α-BH, respectively, in the Cu(1)-bound CBC*BB*B face and are slightly longer than the corresponding Cu···B distance (2.1399(19) Å) for the sole such interaction in **7**. These distances for Cu(2) are comparable to those (Cu···Cu range 2.576(1)−2.6915(8) Å, Cu···B range 2.158(3)−2.234(3) Å) in analogous exo/endo-dicopper derivatives of 11-vertex heteroborane ligands.[23] There is one further feature in the structure of **9** that is worthy of note. In previous studies upon 4,1,6-MC_2B_{10} systems where exo-polyhedral metal fragments are attached via an α-BH in the CBC*B*BB belt,[1,20,21] we have observed that it is B(3) that is preferred. In **9**, however, the exo-copper center is bonded to the *other*, α′-BH, namely, B(10). This is almost certainly a consequence of the differing bonding requirements of the various vertexes M and the effect that this has upon electron density distribution within the cluster.

In its $^{11}B\{^1H\}$ NMR spectrum, compound **9** shows seven resonances in the ratio 1:1:1:2:1:2:2, a pattern that suggests cluster mirror symmetry. Although this is at odds with the structure determined in the solid state, it can readily be explained by the exo-polyhedral copper unit exchanging between the two equivalent CuB_2 faces {Cu(1)B(7)B(10)} and {Cu(1)B(3)B(7)}, a process that is likely to be rapid on the NMR time scale. This, and similar dynamic processes, results in the absence of signals due to B−H→Cu protons in the ^1H NMR spectrum, as was observed for **7** and **8**. The same spectrum, however, does reveal signals for the phenyl groups (δ 7.45−7.20) and a single broad peak for the cage CH protons (δ 4.34), these being in the ratio 30:2, as expected: the presence of only a single cage CH resonance further confirms the time-averaged molecular symmetry. Two separate, broad resonances are seen in the $^{31}P\{^1H\}$ NMR spectrum of **9**, at δ 8.3 and 7.2, and may be attributed to the two different {Cu(PPh_3)} units. These chemical shifts are comparable to those for the same moieties bonded to *nido*-C_2B_9 carborane ligands.[23a,24] However, in the latter species it was observed that solution dynamic processes render the two phosphorus environments equivalent at ambient temperatures, and only upon cooling[23a] or by the introduction of severe steric crowding[24] could this be arrested. It has been suggested[23a] that these processes may involve exchange of the phosphine ligands between the two coppers and/or exchange of the whole {Cu(P)} unit between exo- and endo-polyhedral sites. On the basis of the ^{31}P NMR data, it appears that no such behavior occurs in **9** at room temperature.

The formation of **9** was very surprising, and the mechanism by which it is obtained is not clear. Attempts to prepare the compound rationally from [*nido*-7,9-$C_2B_{10}H_{12}]^{2-}$ and {Cu(PPh_3)}$^+$ (2 equiv) have so far yielded only *closo*-$C_2B_{10}H_{12}$. At present it also cannot be said whether **7** is a precursor to **9**. Intuitively, it seems unlikely that the {*nido*-$C_2B_{10}\}^{2-}$ ligand would dissociate from the rhenium center of **7** (or **2a**) to then be trapped by {Cu(PPh_3)}$^+$. However, the resulting {*closo*-$CuC_2B_{10}\}^-$ group with a further copper fragment would give the observed compound **9**. Conversely, we have recently observed that an 11-vertex manganese-monocarbollide cluster can accept an (exo-polyhedral) platinum fragment and that the resulting {$PtMnCB_9$} intermediate extrudes the manganese vertex, which then itself assumes an exo-polyhedral role.[25] It might be speculated that the {ReC_2B_{10}-*exo*-Cu} compound **7** similarly forms a closed 14-vertex {$ReCuC_2B_{10}$} cluster, which then extrudes rhenium to give a transient {CuC_2B_{10}-*exo*-Re} species, and that the action of further copper thereupon displaces the rhenium to give **9**. Investigations are continuing in an effort to understand the formation of **9** and the conditions that favor its production.

Conclusions

The new metallacarboranes [N(PPh_3)$_2$][4,4,4-$(CO)_3$-*closo*-4,1,6-$MC_2B_{10}H_{12}$] (M = Re (**2a**), Mn (**2b**)) have been prepared. Reaction of **2a** with iodine has provided the first example of *B*-halogenation in 13-vertex {MC_2B_{10}} cage systems. Treatment of the *B*-iodinated compound with a Grignard reagent results in a cross-coupling reaction to form a *B*-alkylated species; by extension of this methodology, a series of similarly derivatized compounds may be envisioned. In addition, the fortuitous *B*-chlorination in the formation of **6** provided C−H···Cl−B interactions in the solid state and hence an unusual crystal packing for this compound. Bimetallic species involving either direct Re−Cu or Re−Au bonds, supported by a B−H→M′ agostic-type interaction, have also been prepared, of which the Re−Au species is notable in that a 12-vertex analogue does not exist at this time. Given the rich chemistry already demonstrated for **1a**[4−6] and **1b**,[2c] these initial studies of the reactivity of **2a** augur well for the further development of the reaction chemistry of 13-vertex metallacarboranes.

Experimental Section

General Considerations. All reactions were carried out under an atmosphere of dry, oxygen-free nitrogen using Schlenk line techniques. Some subsequent manipulations were performed in the air. Solvents were distilled from appropriate drying agents under nitrogen prior to use. Petroleum ether refers to that fraction of boiling point 40−60 °C. Chromatography columns (typically ca. 15 cm in length and ca. 2 cm in diameter) were packed with silica gel (Acros, 60−200 mesh). Filtrations through Celite typically employed a pad 5 cm deep. Preparative thin-layer chromatography (TLC) employed plates of dimensions 200 × 200 mm (silica gel GF_{254}, 250 μm layer, Merck). NMR spectra were recorded at the following frequencies (MHz): ^1H, 360.1; ^{13}C, 90.6; ^{11}B, 115.5; ^{31}P, 145.8. The compounds [$ReBr(CO)_5$],[26] [$Mn(NCMe)_3(CO)_3$][PF_6],[27] [CuCl(PPh_3)]$_4$,[28] and [AuCl(PPh_3)][29] were obtained by literature methods. All other reagents were used as received.

Synthesis of [N(PPh_3)$_2$][4,4,4-$(CO)_3$-*closo*-4,1,6-$MC_2B_{10}H_{12}$] (M = Re, Mn). (i) A Schlenk tube fitted with a

(23) (a) Kang, H. C.; Do, Y.; Knobler, C. B.; Hawthorne, M. F. *Inorg. Chem.* **1988**, *27*, 1716. (b) Thornton-Pett, M.; Kennedy, J. D.; Faridoon; Spalding, T. R. *Acta Crystallogr.* **1995**, *C51*, 840. (c) Thornton-Pett, M.; Kennedy, J. D.; Breen, S. P.; Spalding, T. R. *Acta Crystallogr.* **1995**, *C51*, 1496.

(24) Adams, K. J.; Cowie, J.; Henderson, S. G. D.; McCormick, G. J.; Welch, A. J. *J. Organomet. Chem.* **1994**, *481*, C9.

(25) Du, S.; Jeffery, J. C.; Kautz, J. A.; Lu, X. L.; McGrath, T. D.; Miller, T. A.; Riis-Johannessen, T.; Stone, F. G. A. *Inorg. Chem.* **2005**, *44*, 2815.

(26) Schmidt, S. P.; Trogler, W. C.; Basolo, F. *Inorg. Synth.* **1990**, *28*, 160.

(27) Reiman, R. H.; Singleton, E. *J. Chem. Soc., Dalton Trans.* **1974**, 808.

cooling jacket was charged with $[ReBr(CO)_5]$ (1.52 g, 3.74 mmol) and THF (25 mL), and the mixture was brought to reflux for 16 h, generating $[ReBr(CO)_3(THF)_2]$ in situ.[30] After this time, in a separate Schlenk flask, Na cuttings (ca. 0.25 g, 10.4 mmol) were added to a THF (25 mL) solution of *closo*-1,2-$C_2B_{10}H_{12}$ (0.54 g, 3.74 mmol) and a catalytic amount of naphthalene, and the mixture was stirred until a dark green coloration persisted (ca. 20 min). Excess Na was removed, and into this solution of Na_2[*nido*-7,9-$C_2B_{10}H_{12}$] was transferred (via cannula) the still hot THF solution of $[ReBr(CO)_3(THF)_2]$. The resultant orange mixture was stirred for 2 h. After addition of $[N(PPh_3)_2]Cl$ (2.15 g, 3.74 mmol) and stirring for a further 1 h, volatiles were removed in vacuo, and the resulting residue was extracted with CH_2Cl_2 (30 mL). The extract was reduced in volume to ca. 5 mL in vacuo before being passed down a chromatography column using CH_2Cl_2−petroleum ether (2:1) as eluant to yield a single orange band, which was collected and reduced to dryness, and the residue was washed with petroleum ether (4 × 30 mL) to yield $[N(PPh_3)_2]$[4,4,4-$(CO)_3$-*closo*-4,1,6-$ReC_2B_{10}H_{12}$] (**2a**) (2.1 g) as yellow microcrystals.

(ii) A THF (25 mL) solution Na_2[*nido*-7,9-$C_2B_{10}H_{12}$] was prepared as above from *closo*-1,2-$C_2B_{10}H_{12}$ (0.100 g, 0.69 mmol) and Na cuttings (ca. 0.10 g, 4.35 mmol) and then cooled to −78 °C before addition of $[Mn(NCMe)_3(CO)_3][PF_6]$ (0.42 g, 0.87 mmol). The resultant orange mixture was stirred at room temperature for 2 h. After treatment with $[N(PPh_3)_2]Cl$ (0.40 g, 0.87 mmol) the mixture was worked up in a fashion similar to that for **2a** to yield $[N(PPh_3)_2]$[4,4,4-$(CO)_3$-*closo*-4,1,6-$MnC_2B_{10}H_{12}$] (**2b**) (0.14 g) as a yellow powder.

Synthesis of $[N(PPh_3)_2]$[4,4,4-$(CO)_3$-7-I-*closo*-4,1,6-$ReC_2B_{10}H_{11}$]. To a CH_2Cl_2 solution (15 mL) of **2a** (0.194 g, 0.20 mmol) was added I_2 (0.052 g, 0.20 mmol) and the resultant mixture stirred for 1.5 h. The volume of the solution was reduced to ca. 5 mL in vacuo before being passed down a chromatography column using CH_2Cl_2−petroleum ether (1:1) as eluant to yield a single yellow band. This was collected and reduced to dryness, and the residue was washed with petroleum ether (3 × 20 mL) to yield $[N(PPh_3)_2]$[4,4,4-$(CO)_3$-7-I-*closo*-4,1,6-$ReC_2B_{10}H_{11}$] (**3**) (0.077 g) as a yellow microcrystalline solid.

Synthesis of $[N(PPh_3)_2]$[4,4,4-$(CO)_3$-7-Me-*closo*-4,1,6-$ReC_2B_{10}H_{11}$]. A CH_2Cl_2 solution (15 mL) of **2a** (0.257 g, 0.27 mmol) was treated with I_2 (0.068 g, 0.27 mmol) and the resultant mixture stirred for 1.5 h before removal of volatiles in vacuo. This residue of crude **3** was dissolved in THF (15 mL) and the solution cooled to −78 °C before addition of MeMgBr (2.9 mL, 1.4 M solution in toluene−THF (3:1), 4.06 mmol) and $[PdCl_2(PPh_3)_2]$ (0.019 g, 0.03 mmol). The resultant mixture was allowed to warm to room temperature and stirred for 16 h. Addition of dilute HCl with subsequent separation of the organic layer and removal of solvents in vacuo afforded $[N(PPh_3)_2]$[4,4,4-$(CO)_3$-7-Me-*closo*-4,1,6-$ReC_2B_{10}H_{11}$] (**4**) (0.026 g) as a yellow-brown powder.

Synthesis of [4,4-$(CO)_2$-4-NO-7-X-*closo*-4,1,6-$ReC_2B_{10}H_{11}$] (X = H, Cl). To a cooled (−78 °C) CH_2Cl_2 solution (10 mL) of **2a** (0.250 g, 0.26 mmol) was added $[NO][BF_4]$ (0.091 g, 0.78 mmol) and the resultant mixture stirred for 2 h. The solution was then concentrated and applied to a chromatography column. Elution with CH_2Cl_2−petroleum ether (2:3) gave a broad yellow band. The latter was collected and purified by preparative TLC using the same solvent mixture, yielding two yellow bands, which were collected separately and reduced to dryness in vacuo to yield, respectively, [4,4-$(CO)_2$-4-NO-*closo*-4,1,6-$ReC_2B_{10}H_{12}$] (**5**) (0.024 g) and [4,4-$(CO)_2$-4-NO-7-Cl-*closo*-4,1,6-$ReC_2B_{10}H_{11}$] (**6**) (0.025 g), as yellow microcrystals.

Table 3. Crystallographic Data for Compounds 2, 4, and 6−9

	2a	**2b**	**4**	**6**	**7**	**8**	**9**
formula	$C_{41}H_{42}B_{10}NO_3P_2Re$	$C_{41}H_{42}B_{10}MnNO_3P_2$	$C_{42}H_{44}B_{10}NO_3P_2Re$	$C_4H_{11}B_{10}ClNO_3Re$	$C_{23}H_{27}B_{10}CuO_3PRe$	$C_{23}H_{27}AuB_{10}O_3PRe$	$C_{38}H_{42}B_{10}Cu_2P_2$
fw	953.00	821.74	967.02	450.89	740.26	873.68	795.84
space group	$P2_1/c$	$P2_1/c$	$P2_1/n$	$P1^a$	$P\bar{1}$	$P\bar{1}$	$P2_1/n$
a, Å	11.4867(10)	11.5244(15)	13.9958(10)	7.1474(5)	9.1080(4)	8.973(7)	9.9527(9)
b, Å	17.2181(15)	17.356(2)	21.9350(15)	7.2040(5)	13.0195(5)	12.990(11)	20.7859(19)
c, Å	21.581(2)	21.248(3)	14.3679(10)	14.5058(9)	13.6694(5)	13.750(12)	19.0028(18)
α, deg	90	90	90	86.494(4)	64.507(2)	64.60(5)	90
β, deg	99.684(6)	99.847(6)	103.707(3)	86.862(3)	83.966(2)	84.03(5)	93.238(4)
γ, deg	90	90	90	67.238(3)	71.187(2)	70.23(5)	90
V, Å^3	4207.4(6)	4187.5(9)	4285.3(5)	687.05(8)	1383.88(10)	1361(2)	3924.9(6)
Z	4	4	4	2	2	2	4
ρ_{calcd}, g cm^{-3}	1.504	1.303	1.499	2.180	1.776	2.132	1.347
μ(Mo Kα), mm^{-1}	3.004	0.432	2.951	9.028	5.222	9.913	1.193
no. of reflns measd	111 784	58 418	71 728	37 119	38 202	19 076	58 189
no. of indept reflns	14 842	8337	15 379	16 557	9901	5645	14 595
R_{int}	0.0681	0.0592	0.0394	0.0214	0.0319	0.0353	0.0531
wR2, R1[b] (all data)	0.0787, 0.0581	0.1017, 0.0608	0.0901, 0.0576	0.0639, 0.0287	0.0485, 0.0247	0.0654, 0.0330	0.0971, 0.0628
wR2, R1 (obs[c] data)	0.0723, 0.0341	0.0939, 0.0398	0.0833, 0.0351	0.0634, 0.0257	0.0478, 0.0204	0.0635, 0.0257	0.0890, 0.0390

[a] Absolute structure not determined: the crystal is a racemic twin (see text). [b] $wR2 = [\sum\{w(F_o^2 - F_c^2)^2\}/\sum w(F_o^2)^2]^{1/2}$; $R1 = \sum||F_o| - |F_c||/\sum|F_o|$. [c] $F_o > 4\sigma(F_o)$.

(28) Jardine, F. H.; Rule, J.; Vohra, G. A. *J. Chem. Soc. A* **1970**, 238.

(29) Bruce, M. I.; Nicholson, B. K.; Bin Shawkataly, O. *Inorg. Synth.* **1989**, *26*, 325.

(30) Vitali, D.; Calderazzo, F. *Gazz. Chim. Ital.* **1972**, *102*, 587.

Reaction of Compound 2a with Sources of $\{M'(PPh_3)\}^+$ (M = Cu, Au). (i) To a CH_2Cl_2 solution (10 mL) of **2a** (0.250 g, 0.26 mmol) was added $[CuCl(PPh_3)]_4$ (0.095 g, 0.07 mmol) followed by $Tl[PF_6]$ (0.091 g, 0.26 mmol). After stirring for 4 h the mixture was filtered (Celite) and the filtrate passed down a chromatography column using CH_2Cl_2−petroleum ether (1:1) as eluant to yield a single pale yellow band. This was collected and reduced to dryness, and the residue washed with petroleum ether (3 × 30 mL) to yield [4,4,4-$(CO)_3$-4,7-{Cu(PPh_3)}-7-(μ-H)-*closo*-4,1,6-$ReC_2B_{10}H_{11}$] (**7**) (0.115 g) as a pale yellow, microcrystalline solid.

Occasionally, compound **7** as isolated was observed to contain up to ca. 10% (estimated by integrated ^{11}B NMR spectroscopy) of another metallacarborane product. Unfortunately, the two species resisted chromatographic separation. However, repeated recrystallization of the product mixture (solvent diffusion, CH_2Cl_2−petroleum ether (1:4), −30 °C) afforded pale yellow blocks of **7**, along with a small quantity of very pale yellow prisms of [4-PPh_3-4,7,10-{Cu(PPh_3)}-7,10-(μ-H)$_2$-4,1,6-*closo*-$CuC_2B_{10}H_{10}$] (**9**). A sufficient quantity of the crystals of compound **9** could be separated manually to obtain NMR spectroscopic data and one crystal that was suitable for an X-ray diffraction study.

(ii) Similar to the synthesis of **7** above, addition of [AuCl(PPh_3)] (0.081 g, 0.16 mmol) and $Tl[PF_6]$ (0.057 g, 0.16 mmol) to a CH_2Cl_2 solution (10 mL) of **2a** (0.156 g, 0.16 mmol), with workup as described above, produced [4,4,4-$(CO)_3$-4,7-{Au(PPh_3)}-7-(μ-H)-*closo*-4,1,6-$ReC_2B_{10}H_{11}$] (**8**) (0.055 g) as pale yellow microcrystals.

Structure Determinations. Crystals of all compounds studied were obtained by slow diffusion of petroleum ether into CH_2Cl_2 solutions at −30 °C. Experimental data for all determinations are presented in Table 3. X-ray intensity data were collected at 110(2) K on a Bruker-Nonius X8 APEX CCD area-detector diffractometer using Mo Kα X-radiation. Several sets of narrow data "frames" were collected at different values of θ, for various initial values of ϕ and ω, using 0.5° increments of ϕ or ω. The data frames were integrated using SAINT;[31] the substantial redundancy in data allowed an empirical absorption correction (SADABS)[31] to be applied, based on multiple measurements of equivalent reflections.

All structures were solved using conventional direct methods[31,32]—with the exception of **2a**, which was solved from the Patterson function—and refined by full-matrix least-squares on all F^2 data using SHELXL-97.[32] The locations of the cage-carbon atoms were verified by examination of the appropriate internuclear distances and the magnitudes of their isotropic thermal displacement parameters. All non-hydrogen atoms were assigned freely refining anisotropic displacement parameters. The sole exception to this was the structure of **2a**, in which there was some significant disorder associated with B(5). This necessitated restraint of this atom toward isotropic behavior (ISOR card in SHELXL[32]). Similar difficulties have been reported in the structural determination of related 13-vertex metallacarborane species.[14]

All carborane H atoms, including those involved in B−H⇀M agostic-type interactions, were located in difference maps, and the majority were allowed free positional refinement; however, a few such hydrogens did not retain sensible positions upon refinement and the process was assisted by use of the DFIX or AFIX cards in SHELXL,[32] as was deemed appropriate. The hydrogen atoms in organic groups were included in calculated positions and allowed to ride on their parent atoms. All H atoms were assigned fixed isotropic thermal parameters, calculated as $U_{iso}(H) = 1.2 \times U_{iso}$(parent) or $U_{iso}(H) = 1.5 \times U_{iso}$(parent) for methyl hydrogens.

Compound **6** crystallizes in the noncentrosymmetric space group $P1$, with two crystallographically independent molecules per asymmetric unit. Each of the two sets of independent molecules is involved in weak hydrogen-bonding interactions that utilize a cage C−H unit as donor and the chloride atom on an adjacent cluster as acceptor (see discussion in text). The directionality and orientation of molecules within the hydrogen-bonded sets preclude the presence of crystallographic symmetry and hence the reasonable space group assignment. Molecules of **6** are chiral but, of course, would be formed as the racemate. The crystal itself, however, formed as a racemic twin, and hence no absolute structure information could be obtained from this determination.

Acknowledgment. We thank the Robert A. Welch Foundation for support. The Bruker-Nonius X8 APEX diffractometer was purchased with funds received from the National Science Foundation Major Research Instrumentation Program (Grant CHE-0321214).

Supporting Information Available: Full details of crystallographic analyses as a CIF file. This material is available free of charge via the Internet at http://pubs.acs.org.

OM050226G

(31) *APEX 2*, version 1.0; Bruker AXS: Madison, WI, 2003−2004.
(32) *SHELXTL* version 6.12; Bruker AXS: Madison, WI, 2001.